

1 **CASE STUDY: A RAPID URBAN INUNDATION FORECASTING TECHNIQUE**
2 **BASED ON QUANTITATIVE PRECIPITATION FORECAST FOR HOUSTON AND**
3 **HARRIS COUNTY FLOOD CONTROL DISTRICT**

4 Shahryar Ahmad, Md. Safat Sikder and Faisal Hossain– University of Washington, Seattle, WA

5 Abebe S. Gebregiorgis – Harris County Flood Control District, Houston, TX

6 Hyongki Lee – University of Houston, Houston, TX

7 **Abstract**

8 This research explored the operational feasibility of quantitative precipitation forecasting (QPF)
9 using high resolution numerical weather prediction models at the urban landscape scale for flood
10 inundation forecasting in the city of Houston for Harris County Flood Control District (HCFCD).
11 The authors propose and test a rapid-refresh technique for generating forecasted flood inundation
12 maps. The time required to process such maps for an urban flood management agency is
13 controlled only by the time required for generating high resolution QPF. The study investigated
14 hurricane (e.g. Harvey) and non-hurricane type storms. Using the dense gauge network operated
15 by the HCFCD, it was found that hurricane type storms are generally more challenging for
16 precipitation forecasting than the less intense and more frequent winter storm events. The
17 investigation of gauge-based water level measurements indicated that it is possible to forecast
18 inundation level at water level gauging points based on rainfall forecast using pre-developed
19 rating curves between forecast rainfall and expected increase in water level. Using this rating
20 curve approach, it was found that the median of relative RMSE (percentage) and correlation of
21 forecasted water level at gauge locations are consistently below 10% and higher than 0.7,
22 respectively for up to 4 day of lead-time, subject to availability of adequate computational

23 resources. In terms of spatial detection of flooded (non-flooded) areas, our technique yields
24 qualitative consistency during peak inundation episodes in Houston at 1 day of lead-time when
25 compared against satellite radar imagery or in-situ based technique. In general, it is found that
26 flood inundation forecast accuracy during peak episodes is not as compromised as QPF skill for
27 hurricane-strength storms, indicating that the highly urbanized nature of Houston is more ideally
28 suited for inundation mapping using the rating curve approach.

29 **Keywords:** Houston, urban flooding, hurricane, Harris County, Harvey, forecasting, WRF

30

31

32 **1. INTRODUCTION**

33 Houston has frequently experienced the nation’s worst urban flooding events (Zelinski
34 and Zaveri 2018). With its flat and saucer-like terrain, highly urbanizing landscape, inadequate
35 storm drainage capacity and intense precipitation events, there is no doubt that Houston will
36 experience urban flooding in the foreseeable future. For example, in one study using remote
37 sensing imagery of land cover, asphalt and concrete increased 21% during 1984–1994, 39% in
38 1994–2000 and 114%, from 2000 to 2003, while vegetation suffered an overall decrease (Khan
39 2005). Such rapidly urbanizing landscape appears more alarming when considered in the context
40 of recent studies on projected trends of extreme rainfall for the state of Texas. One study
41 estimated that the annual probability of a 500 mm of area-integrated rainfall was about 1% in the
42 period 1981–2000 and that this is likely to increase to 18% over the period 2081–2100 under
43 Intergovernmental Panel on Climate Change (IPCC) AR5 representative concentration pathway
44 8.5 (Emanuel 2017). Furthermore, if it was assumed that the frequency of such events increases
45 linearly in time, then an event like Hurricane Harvey probably had a 6% chance of occurrence in
46 2017, which is a six-fold increase since the late 20th century (Emanuel 2017).

47 Given this increasing propensity for Houston to frequently experience more catastrophic
48 urban flooding, it is opportune time to explore the operational potential of quantitative
49 precipitation forecast (QPF) from numerical weather prediction (NWP) models for real-time
50 urban flood management. QPF can be considered a low-hanging fruit that is freely available to
51 any agency for real-time forecasting of weather events (e.g. Liguori et al. 2012, Liu et al. 2015).
52 The goal here was to understand the operational sustainability of using the publicly available and
53 real-time QPF produced by the National Oceanic and Atmospheric Administration (NOAA)
54 Global Forecasting system (GFS). This research studied the hurricane strength extreme storm

55 Harvey and lesser magnitude events. Since, GFS-based weather forecasts available at a high
56 frequency are available at a coarse spatial resolution of 0.25 degree (25 km), dynamic
57 downscaling to higher spatial resolution (1 km) using a cloud resolving NWP model is necessary
58 for flood forecasting at the urban landscape scale (Chen and Hossain 2016, Sikder and Hossain
59 2016).

60 In order to explore a sustainable operational strategy for rapid forecasting of flood
61 inundation, the authors engaged closely with Harris County Flood Control District (HCFCD),
62 which is the main agency with the mandate for urban flood management for the city of Houston.
63 Towards this goal, this study posed the following research questions:

- 64 1. How does skill of high resolution QPF vary as a function of lead time for Harvey and
65 non-Harvey type extreme storm events over Houston?
- 66 2. Can high resolution QPF be used for water level/inundation forecasting?
- 67 3. What is a feasible and sustainable approach for HCFCD (and similar agencies) to take
68 advantage of high resolution QPF in urban flood disaster management?

69 **2. THE SELECTED STORMS**

70 Two storm events were selected in this study. The first storm was Hurricane Harvey,
71 while the second one was of a lesser magnitude (with a typical 2-year return period). In both
72 cases, the specific date was selected, when rainfall (hereafter interchangeably used with
73 precipitation) total was maximum as the target date for forecasting up to 96 hours ahead of time
74 (i.e., 4-day lead-time). The specific peak rainfall dates for the storms are:

75 **Harvey storm** – August 26, 2017 (daily and areal averaged rainfall total= 276 mm)

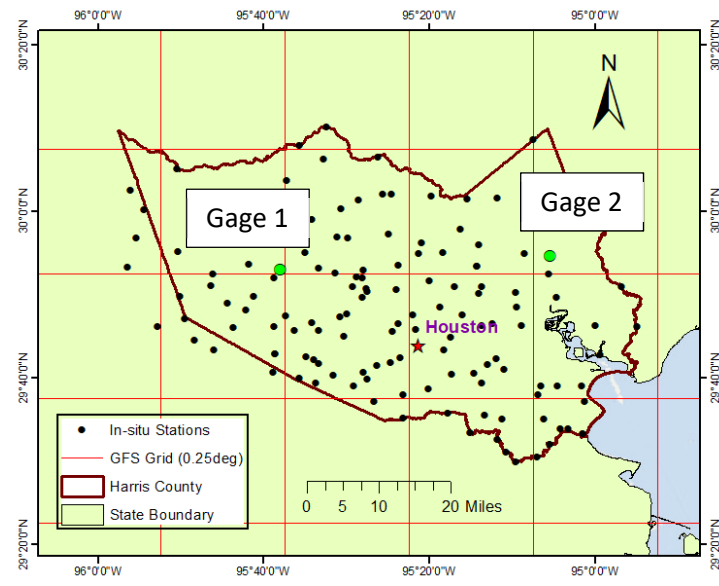
76 **Non-Harvey Class storm** – February 21, 2018 (daily and areal averaged rainfall total= 25 mm)

77 Another Non-Harvey storm event was selected for further analysis in this study, which had the
78 maximum magnitude on January 18, 2017 (daily and areal averaged rainfall total= 65 mm). This
79 storm event along with the above two events were used to develop the precipitation-water level
80 rise relation (i.e., rating curve), which later used to generate the water level forecast.

81 3. DATA AND MODELS

82 3.1 In-Situ Rainfall and Water Level Data

83 Harris County Flood Control District has a very dense rainfall gauge and water level
84 monitoring network. For ground rainfall data, the authors had access to 139 recording gauges
85 distributed in the county with an average density of 1 gauge in a 5X5km grid. Figure 1 shows the
86 location of these gauges that transmitted rainfall and water level every 5 minutes to HCFC
87 headquarters via a telemetered network.



88
89 **Fig. 1.** Location of HCFCDF rainfall and water level gauges in the county where Houston is
90 located. The larger grids are 25 km in size and typical size for NOAA’s QPF (GFS). Location of
91 two selected gauges are shown as green to demonstrate the response of water level change to
92 precipitation spells in figure 5.

93 **3.2 The Global Forecasting System (GFS) for NWP Forecasts**

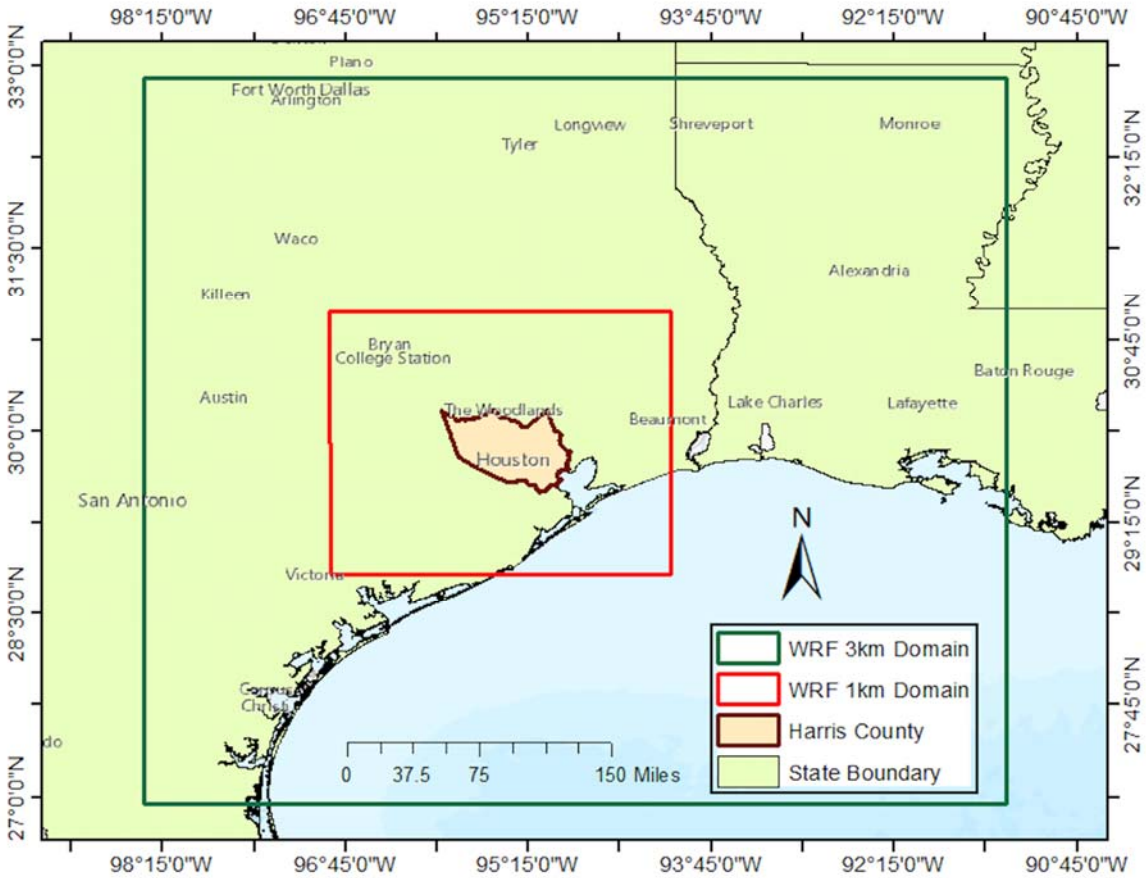
94 The Global Forecasting System (GFS) developed by the National Oceanic and
95 Atmospheric Administration (NOAA) was used as the key source of NWP model based QPF.
96 GFS produces global-scale weather forecast up to 16 days lead time at a spatial resolution
97 ranging from 0.25 degree to 1 degree. This is perhaps the only publicly available weather
98 forecast at a global scale for operational use. The motivation for exploring the GFS forecast is
99 further based on the authors' previous experience and success in operational flow forecasting for
100 South and Southeast Asian agencies (Sikder and Hossain 2018, Sikder and Hossain 2016). As a
101 publicly available and real-time product for the world, GFS is therefore ideal for short-term
102 weather prediction applications, particularly in urban flood management agencies that
103 traditionally do not use such modern atmospheric science based solutions. The historical and
104 real-time data are available from National Center for Environmental Information (NCEI) at
105 <https://www.ncdc.noaa.gov/data-access/model-data/model-datasets/global-forecast-system-gfs>.
106 For first 10 days of lead time, the GFS provides forecasts for every 3 hours, and the outputs are
107 available at 0.25, 0.5, 1.0, and 2.5 degree resolutions.

108 **3.3 The Weather Research and Forecasting (WRF) Model**

109 The Weather Research and Forecasting (WRF) model V3.7.1 was used for dynamic
110 downscaling of coarse resolution global NWP weather forecasts, such as from GFS. Such
111 physical downscaling can generate high resolution precipitation forecast over an urban landscape
112 that requires flood inundation model at a very high spatial resolution (in this case 1 km grids).
113 WRF is a mesoscale cloud resolving NWP model, which is the successor of the MM5 model. It
114 uses non-hydrostatic Euler equations, which are fully compressible in nature. WRF offers
115 various features like advanced dynamics, physics, and numerical schemes. For computation, the

116 model uses Arakawa-C grid staggering for horizontal discretization, and second or third order
117 Runge-Kutta integration scheme for time separation. WRF uses terrain-following pressure
118 coordinate system. Thus, the upper boundary of the model maintained by a constant pressure
119 level. Further description of WRF physics and dynamics can be found in Skamarock et al. 2008.

120 Since the focus in this study was on urban scale flooding triggered by extreme storm
121 events, the initial WRF setup used in this study was based on a previous study optimized for
122 simulating urban precipitation event during the Nashville 2010 flood (Chen et al. 2017a).
123 Previous studies suggest that WRF performance is mostly affected by the choices of cloud
124 microphysics and cumulus parameterization schemes (Chen et al. 2017a). Model resolution and
125 initial/boundary conditions (IC/BC) also affect the simulation quality. However in this case, as
126 the goal is to enable real-time forecasting, the GFS forecast fields were used as Initial and
127 boundary conditions. The initial model configuration further refined in this study, based on
128 extensive sensitivity studies for various parameterizations, carried out earlier for heavy storms in
129 the US (reported in Chen and Hossain 2016). Based on these extensive sensitivity studies to
130 identify the optimal WRF configuration, a two-way nesting with three domains (9km-3km-1km)
131 was selected with Morrison microphysics and Kain-Fritsch cumulus schemes (Figure 2).



132

133 **Fig. 2.** WRF nested domain set up over Houston and Harris County. The inner domain has a grid
 134 spacing of 1 km and covers all of HCFCD’s jurisdiction, while the outer domain has spacing of
 135 3km.

136

137 **4. CPU RESOURCES AND COMPUTATIONAL RUN TIME**

138 For operational (real-time) urban flood management, time is of the essence for any
 139 agency. Any forecast must be generated significantly faster than the natural evolution of the
 140 flooding so that the forecasts can be analyzed, processed and disseminated with considerable
 141 lead time to make appropriate decisions. Since, QPF generation using high-resolution NWP
 142 models can be computationally prohibitive; this study was performed on affordable CPU
 143 resources of varying hardware configurations that are likely to be operationally sustainable in the

144 HCFCFCD work environment. In particular, the computational run time was tested on the following
145 CPU configurations:

146 MACHINE 1 (price: 4000 USD): 32 core Intel Xeon 2.4 GHz Linux Workstation

147 MACHINE 2 (price: 3000 USD): 24 core Intel Xeon 2.4 GHz Linux Workstation

148 MACHINE 3 (price: 2000 USD): 12 core Intel Xeon 2.4 GHz Linux Workstation

149 The CPU run time on various machines are shown in Table 1 as a function of lead time.

150 **Table 1.** The CPU run time for 1 day and 4 day (96 hour) lead times

Lead	MACHINE 1	MACHINE 2	MACHINE 3
1 day only	7 hrs	7.5 hrs	20 hrs
4 days (96 hrs) total	28 hrs	30 hrs	80 hrs

151

152 Assuming that a CPU machine worth 4000 USD with 32 cores can be sustainably
153 maintained by a flood agency like HCFCFCD, it appears that generating forecasts only for the 72
154 hour lead time (or longer) would be meaningful due to the runtime of 7 hours per lead day. It
155 should be noted that the computational efficiency of the WRF downscaling can be optimized
156 further through a Graphics Processor Unit (GPU) or parallel version of WRF that runs an order
157 faster. In addition, the inner domain resolution of 1km and outer domain resolution of 3km could
158 be relaxed and assessed of the precipitation forecast skill in a manner similar to the author's
159 previous studies with Nashville 2010 flood (Chen et al. 2017a) or other extreme events studied
160 for Probable Maximum Precipitation in Chen and Hossain (2016). Finally, if flood control
161 districts like HCFCFCD are willing to invest modestly in cloud-based high performance based
162 computing infrastructure (with some of the costs transferred to users of forecasts), it is quite

163 feasible to generate these forecasts in timescales of 30 minutes to an hour each instant an update
164 is needed.

165 **5. SKILL OF HIGH RESOLUTION QUANTITATIVE PRECIPITATION FORECAST**

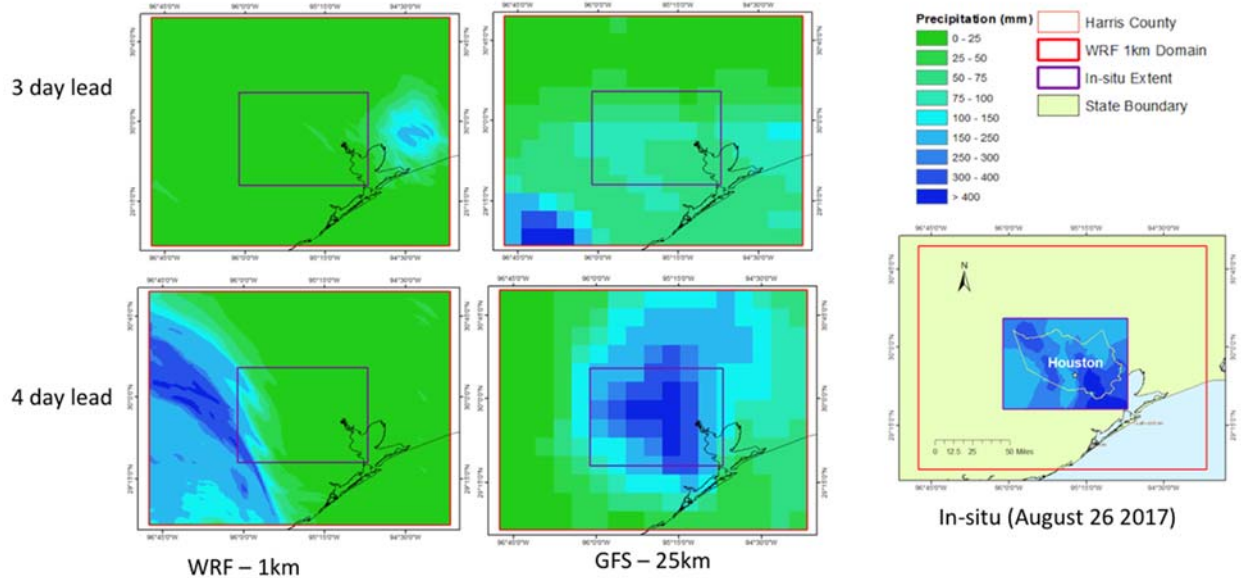
166 **5.1 HURRICANE HARVEY (AUGUST 2017)**

167 Figure 3 shows the rainfall forecast up to 4 day lead time at 25 km (GFS) and 1 km
168 (WRF downscaled) resolution over Harris County. Table 2 summarizes the performance metrics
169 of the forecasted rainfall. It is clear from the assessment that hurricane-strength storms like
170 Harvey are somewhat challenging to forecast unless adequate attention is given to the storm-
171 specific WRF set up. Dynamic downscaling with WRF does not seem to add value to GFS
172 forecast. This is not entirely surprising as past studies have reported on the general difficulty of
173 simulating precipitation during Hurricanes (Emanuel 2017, Rotunno et al. 2008). However, it
174 appears that given sufficient investigation of the choice of WRF model variants, one might be
175 able to simulate high-resolution precipitation forecast at the urban scale for Hurricane events. For
176 example, Dodla et al. 2011 had studied the life cycle of Hurricane Katrina using three variations
177 of the high-resolution WRF model. One particular variation was Hurricane WRF (HWRF)
178 designed specifically for hurricane studies while the other two WRF models had different
179 dynamic cores. For Katrina, the HWRF exhibited superior performance in tracking the evolution
180 of the Hurricane.

181 The specific WRF high resolution NWP model used in this study was derived based on
182 an atmospheric river event (Durkee et al. 2012) that flooded Nashville city in 2010. Due to
183 differing dynamics behind the precipitation process, the choice of cumulus and cloud

184 microphysics parameterizations need to be revisited and calibrated uniquely for Harvey class
 185 storms within perhaps HWRF if the forecast skill is to be further improved.

HARVEY (August 26, 2017)



186

187 **Fig. 3.** Rainfall forecast for Hurricane Harvey on August 26, 2017; Left panel is the downscaled
 188 forecast using WRF at 1 km while right panel is the 25 km scale GFS forecast. The in-situ
 189 rainfall map is shown on the rightmost side and is based on all the gauges of HCFCF.

190 **Table 2.** Skill metrics for rainfall forecast of Hurricane Harvey on August 26, 2017. The metrics
 191 were calculated over the inner domain of WRF that included all 139 gauges. The % is the RMSE
 192 normalized by total precipitation and expressed as a percentage.

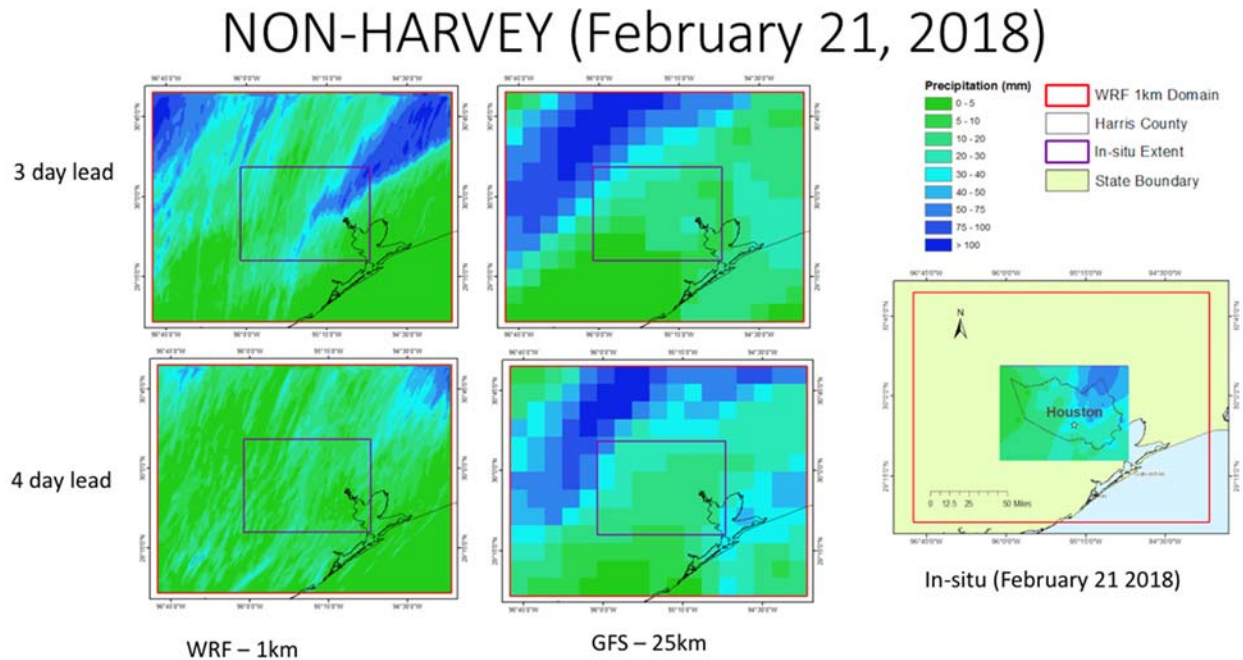
Lead time (hrs)	RMSE (mm)		Correlation		Rainfall Total (mm)		
	WRF	GFS	WRF	GFS	WRF	GFS	In-situ Total
24	96.84 (35%)	172.01 (63%)	-0.012	-0.346	269.50	140.42	276.00
48	222.14 (79%)	178.62 (64%)	-0.282	-0.364	75.58	126.18	276.00
72	275.74 (100%)	222.91 (80%)	0.264	-0.005	8.41	64.46	276.00
96	262.20 (95%)	114.80 (42%)	-0.302	0.112	35.52	274.98	276.00

193

194

195 **5.2 NON-HARVEY STORM (FEBRUARY 2018)**

196 Figure 4 with Table 3 show the rainfall forecast and skill metrics, respectively for a non-
197 Harvey type storm that registered peak rainfall on February 21, 2018. It is clear that non-
198 Hurricane (that are less intense and more frequent) storms have better skill in forecasting using
199 the WRF set up ‘as is’ from Chen et al. 2017a. Furthermore, dynamic downscaling using WRF
200 clearly adds value to GFS forecast. Strong correlation, acceptable percentage RMSE and
201 Probability of Detection at 72 hours lead-time appear to indicate the 72-hour lead-time is an ideal
202 time horizon for forecasting for HCFCD. With further calibration of WRF model similar to Chen
203 and Hossain 2016 or Chen et al. 2017b by selecting appropriate parameterizations for winter
204 precipitation, the WRF setup for Houston should yield skill improvement.



205
206 **Fig. 4.** Same as Figure 3, but for a non-hurricane storm that took place February 21, 2018.

207
208
209

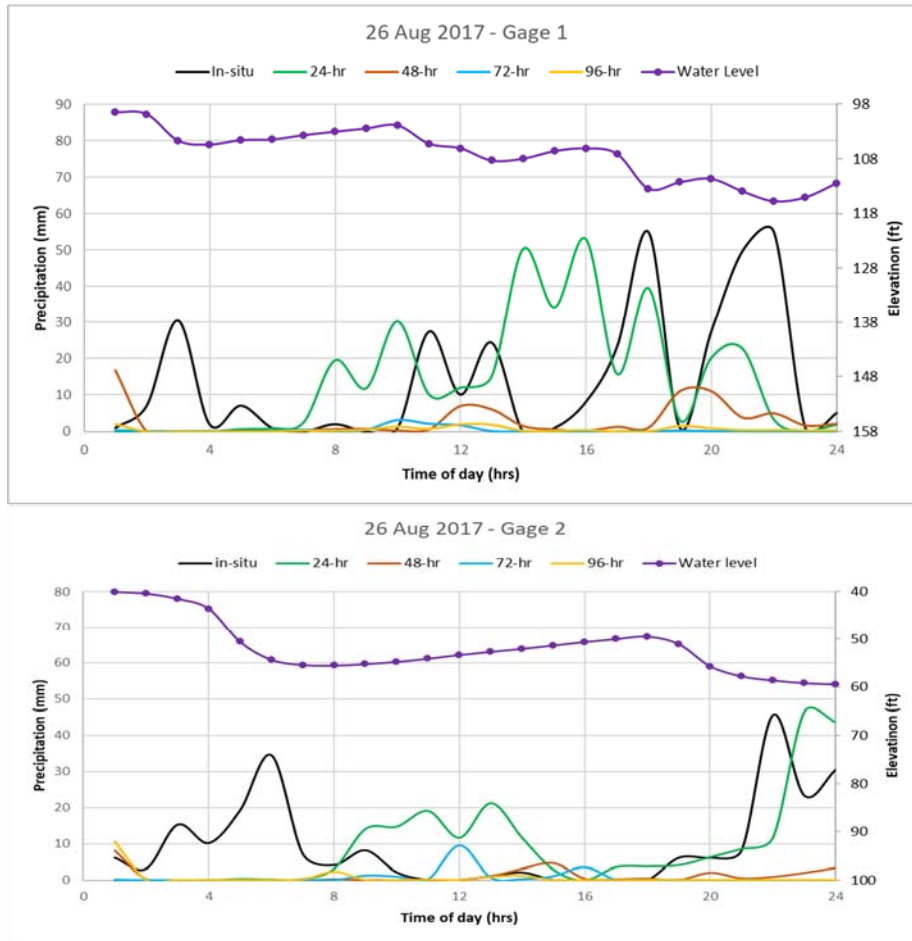
210 **Table 3.** Skill metrics for rainfall forecast of non-Harvey storm date of February 21, 2018. The
 211 metrics were calculated over the inner domain of WRF that included all 139 gauges. The
 212 percentage for RMSE is the RMSE normalized by in-situ precipitation total and expressed as a
 213 percentage.

Lead time (hrs)	RMSE (mm)		Correlation		Rainfall Total (mm)		
	WRF	GFS	WRF	GFS	WRF	GFS	In-situ Total
24	14.95 (59%)	21.02 (84%)	0.38	0.66	26.74	43.24	25.00
48	19.75 (79%)	39.24 (150%)	-0.011	-0.34	17.28	34.84	25.00
72	15.62 (62%)	21.23 (84%)	0.62	-0.14	22.40	14.73	25.00
96	22.26 (89%)	17.78 (71%)	0.20	-0.19	7.59	20.57	25.00

214

215 6. RAPID FLOOD INUNDATON FORECASTING

216 Using the current WRF set up, water level forecasting based on rainfall forecast was
 217 explored. Since, each rainfall gauge also had a water level gauge, the response of water level to
 218 rainfall spells in the same region was studied. Assuming that almost all the rainfall transforms as
 219 urban runoff due to the highly impervious landscape and high rainfall rates, the water level
 220 should in principle be forecastable based on precipitation forecast alone. To explore this idea,
 221 two gauge locations were randomly selected to study the rainfall-water level change co-
 222 variability for nowcast and forecast rainfall (Figure 5; see figure 1 for location). The rainfall here
 223 is the accumulation over the specific WRF 1X1km grid cell and not the drainage area of the
 224 gauge location.



225

226

227 **Fig. 5.** Water level (right axis) variation against precipitation spells (in-situ and forecast for
 228 August 26 2017 (Hurricane Harvey). Locations of gages 1 and 2 can be found in Figure 1.

229

230 It is clear from Figure 5 that water level rise at a point in a stream is triggered strongly by

231 the short precipitation spells at that location, and it is most likely due to most of the rainfall

232 transforming as urban runoff. To explore this phenomenon further for the entire city of Houston,

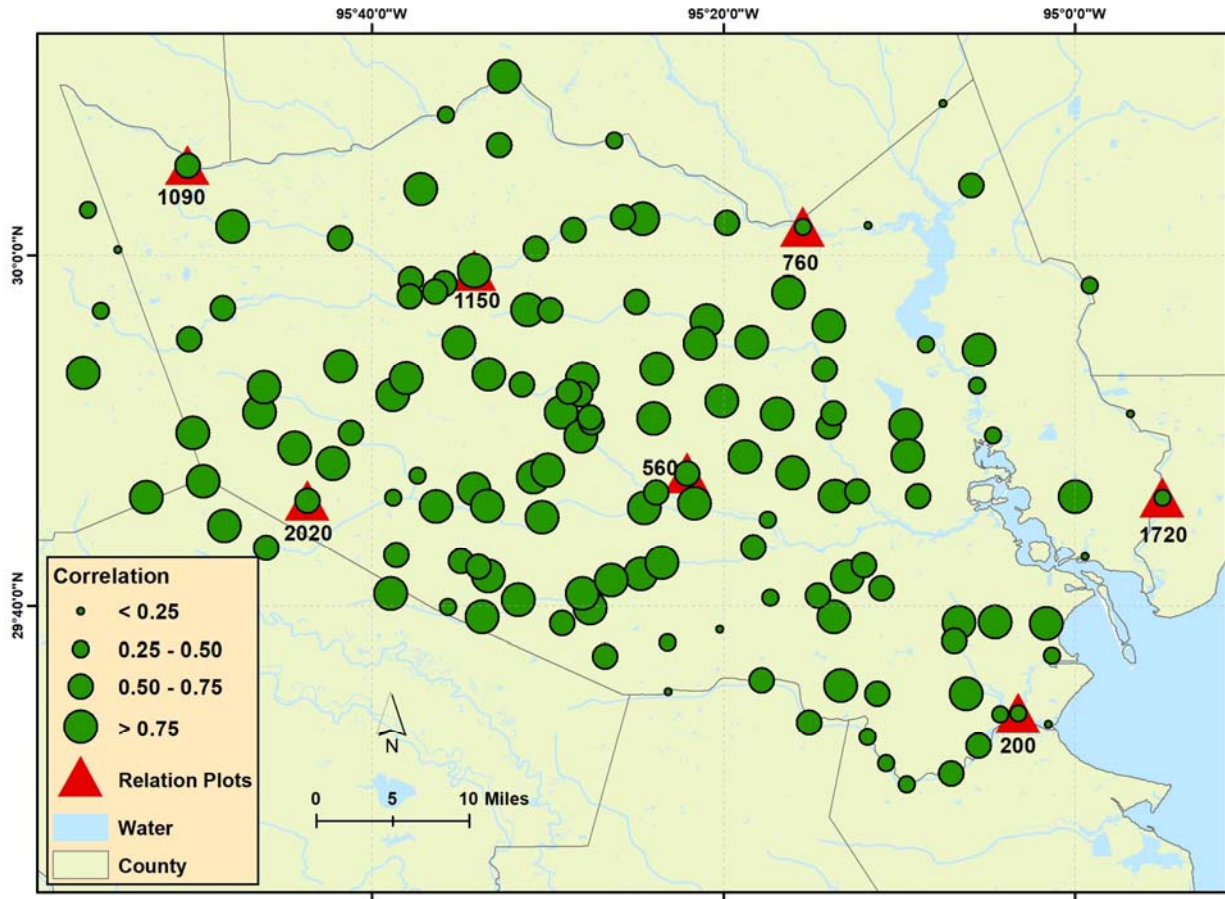
233 the rainfall and water level changes were analyzed at all the locations over multiple storms.

234 Figure 6 shows a map of correlation between in-situ rainfall and in-situ water level increase in

235 water level for the 139 locations in Houston. Figure 7 shows empirical rainfall versus water level

236 increase response at select locations of Figure 6 shown as red triangles.

237

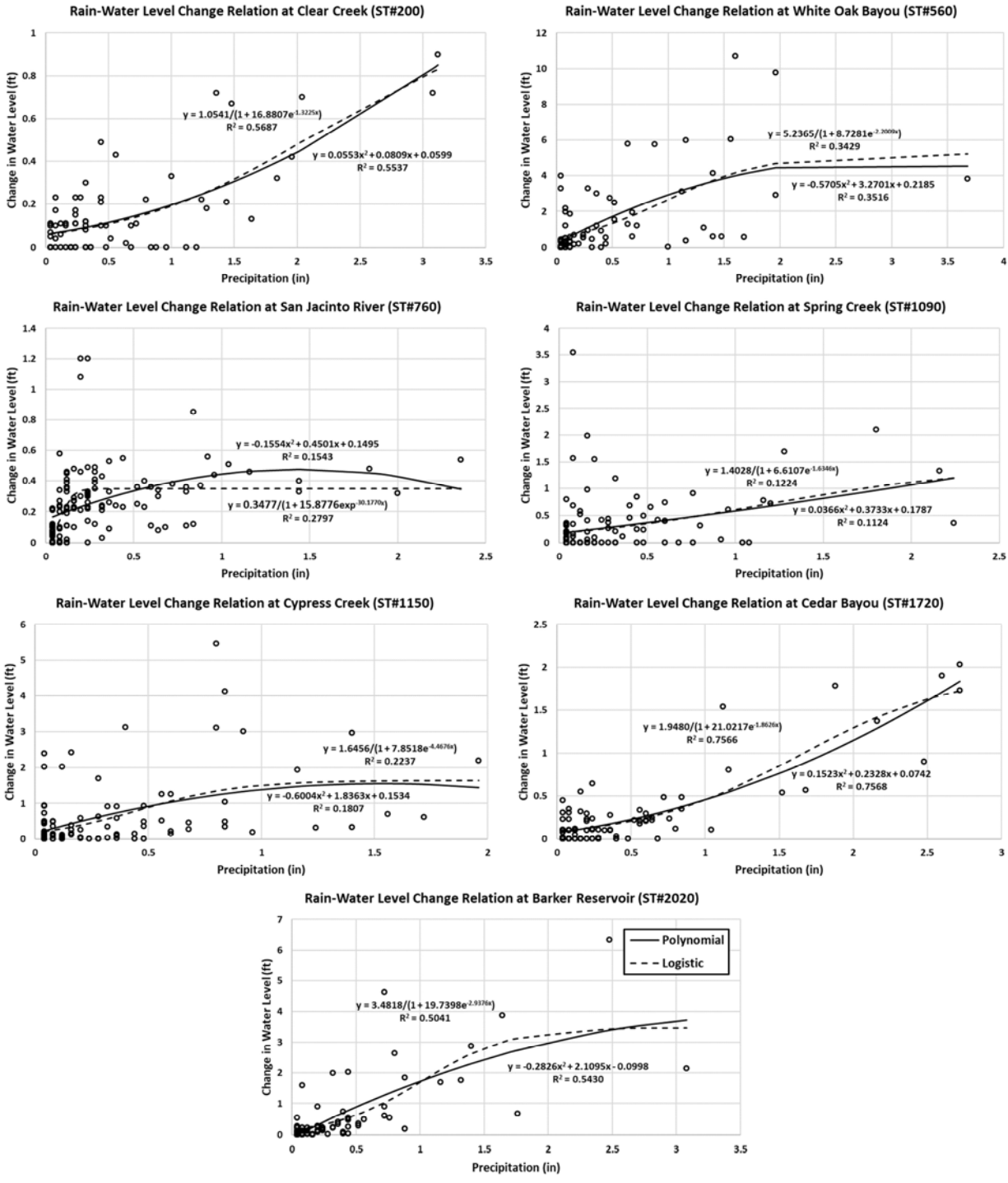


239

240 **Fig. 6.** Correlation between in-situ rainfall and water level increase (from in-situ gauges) at all
 241 the gauge locations of HCFCD over multiple storms. The size of the circle is proportional to the
 242 correlation. The empirical rainfall versus water level increase relationship are shown for
 243 locations shown as red triangles in Figure 7.

244

245 Since, almost every gauge location showed strong covariance between rainfall and
 246 runoff, rating curves were established for each location using in-situ record. This rating curve
 247 essentially predicted the water level increase for a given amount of rainfall. The initial
 248 investigation revealed that a non-linear regression model (such as the logistic or polynomial
 249 equation) was more robust than a linear rating curve in capturing the expected water level

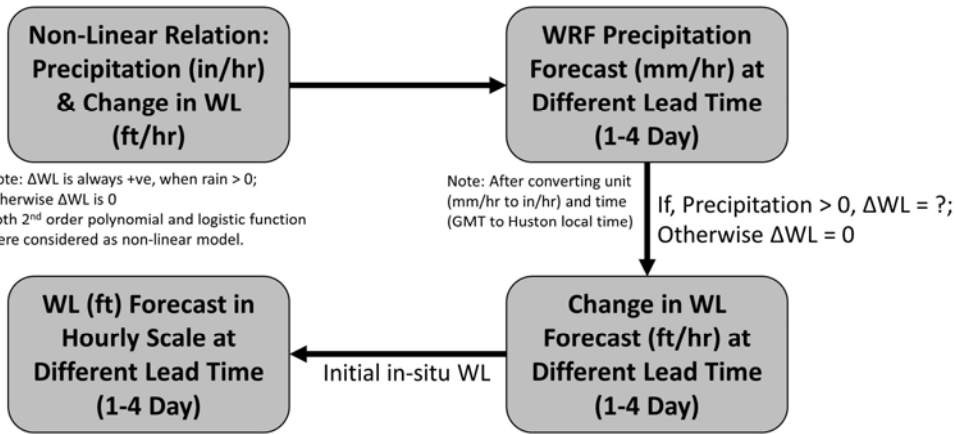


250

251 **Fig. 7.** Empirical relationship between in-situ rainfall and water level increase at in-situ gauges
 252 for selection locations in Houston.

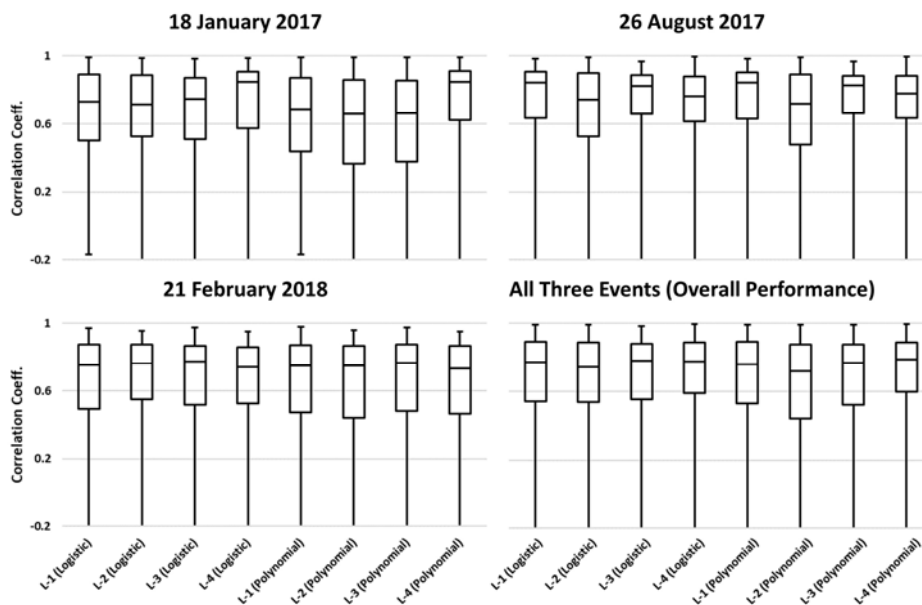
253

254 increase at a location. Using these rating curve relationships developed for each of the 139
 255 locations based on in-situ data, the forecasted rainfall was used to forecast corresponding water
 256 level increase (forecast) for Harvey and non-Harvey storms. The forecasted water level increase
 257 from the rating curves was added with the latest available in-situ water level to predict the water
 258 level at that location for different lead times (i.e., 1-4 day lead). The forecasted water levels were
 259 then assessed of its skill against in-situ water level. For example, to forecast the water level after
 260 24 hours, the forecasted water level change within the next 24 hours was added to the in-situ
 261 nowcast water level at the beginning of 24 hours. Similarly, to forecast the water level after 48
 262 hours, the forecasted water level change within the next 24-48 hours was added to the forecasted
 263 water level after 24 hours, and so on for 72 and 96 hours of lead-times. This approach of
 264 applying a rating curve to generate forecasted water level is summarized in Figure 8 as a
 265 flowchart. It was assumed that the water level will only increase in a location if there is any
 266 precipitation, otherwise the change in water level will be zero. Therefore, this approach is only
 267 valid of a storm event as the storm is intensifying and not when precipitation has already ended,
 268 since there is no decrease in water level.

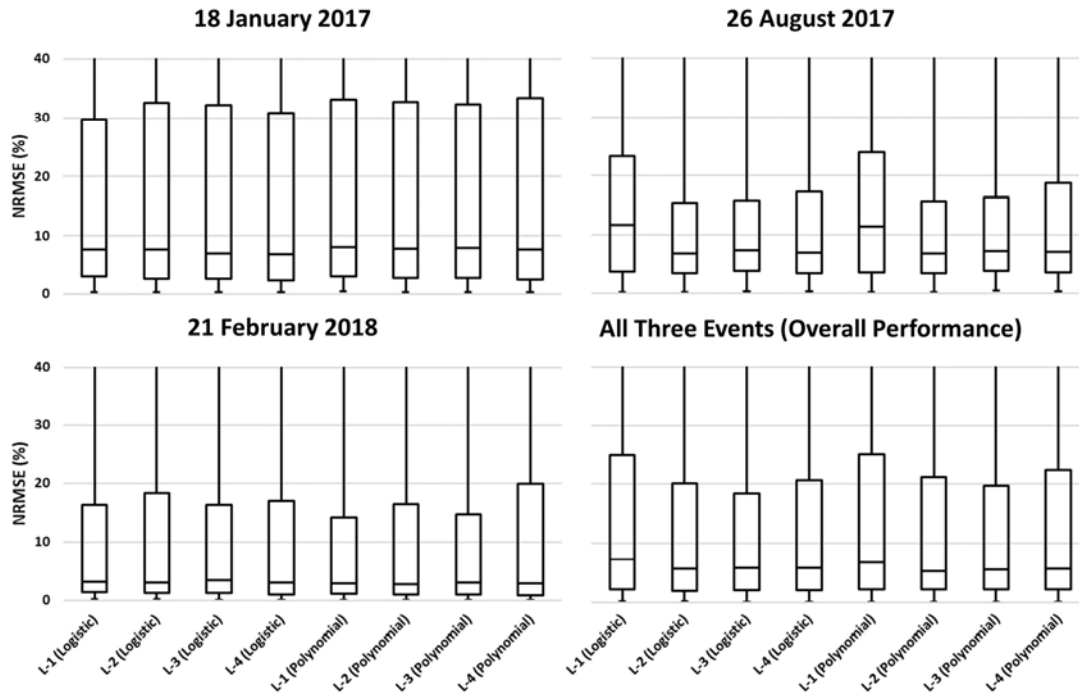


269
 270 **Fig. 8.** Workflow for generating forecasted water level at each of the 139 locations using the pre-
 271 developed rating curves and QPF.

272 Figures 9 and 10 show the skill of water level forecast as a function of lead time and
 273 choice of equation for rating curve for Harvey and non-Harvey storms in terms of correlation and
 274 normalized RMSE, respectively. High skill at correlation (> 0.7) and low NRMSE ($< 10\%$) is
 275 maintained even after lead-time of 96 hours (4 days) although the spread or variability across the
 276 139 gauges is often wider. The fact that forecast water level is better than forecast rainfall even
 277 for hurricane type storms should not be entirely surprising. The contributing runoff leading to the
 278 water level at a location benefits from a highly urbanized drainage where almost all rainfall
 279 becomes runoff and likely cancels the errors in precipitation forecast. For a flood control district
 280 like HCFCD, this is a welcome finding as the proposed rating curve approach to forecasting
 281 inundation is rapid as it can be completed as soon as QPF runs are complete and converted into
 282 maps. Since, the application of a CPU-intensive two dimensional flood inundation model (like
 283 HEC RAS 2D) is not needed, an agency like HCFCD can generate such forecasted inundation
 284 maps as frequently as needed when new precipitation forecasts are available.



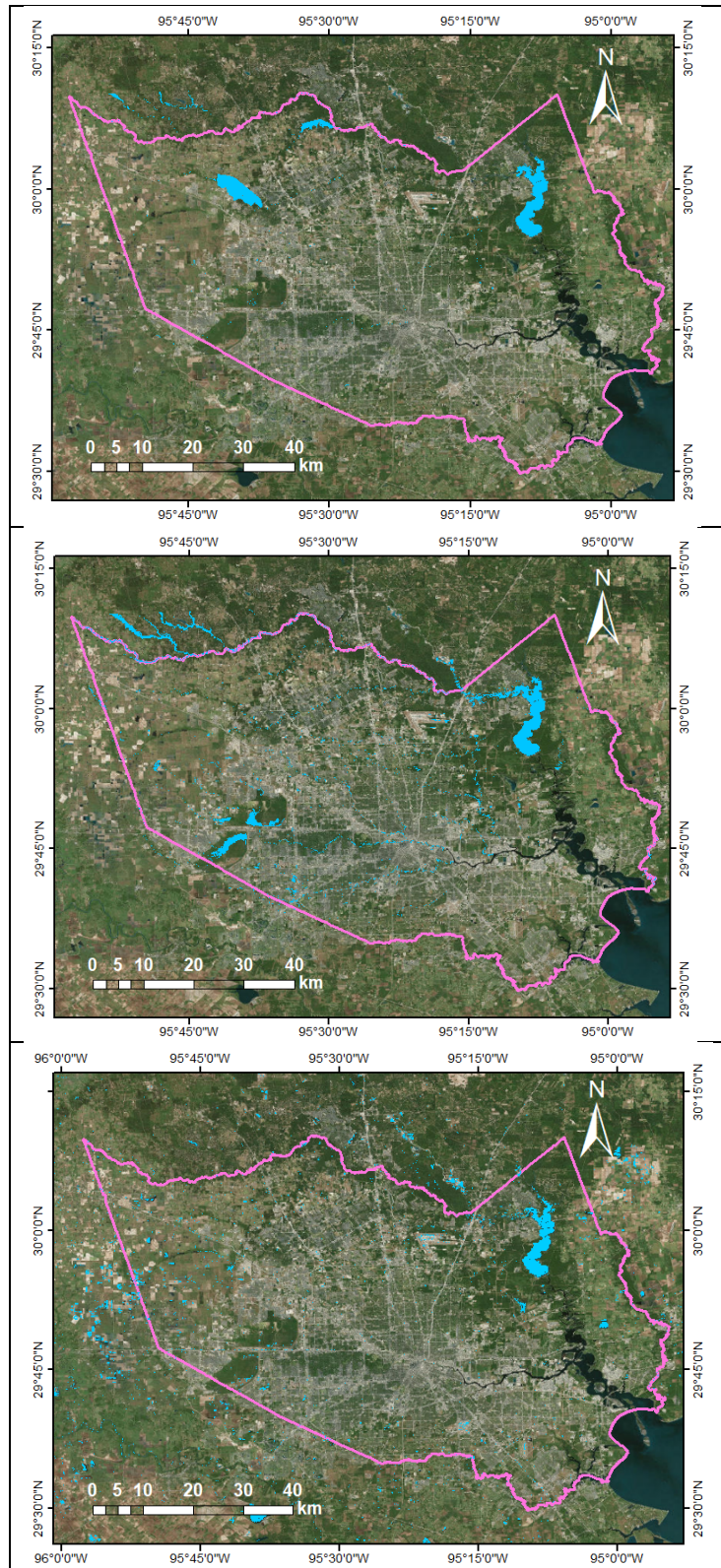
285 **Fig. 9.** Correlation of forecasted water level as a function of lead time and rating curve equation
 286 type (logistic and polynomial) for 3 storms. The correlation is aggregated over all the 139 gauge
 287 locations.
 288



289
 290 **Fig. 10.** Normalized RMSE of forecasted water level (normalized to actual water level) as a
 291 function of lead time and rating curve equation type (logistic and polynomial) for 3 storms. The
 292 correlation is aggregated over all the 139 gauge locations.
 293

294 In Figure 11 the forecasted inundation map is compared with a satellite radar imagery
 295 from Sentinel-1 that overpassed Houston a day later. The same map is also compared with the
 296 map produced using in-situ water levels from HCFCD. The idea here is to explore the spatial
 297 consistency and value of the inundation that is being forecasted here while recognizing that the
 298 flood maps produced in this way are limited to the density of water level gauges. In general, the
 299 spatial consistency seems reasonable when compared with Sentinel-1 or in-situ mapping
 300 technique.

301



302 **Fig. 11.** Comparison of forecasted flood inundation map for Jan 18, 2017 at 1 day lead time
 303 (topmost pane) with observed in-situ gauge based inundation map (middle panel) and satellite
 304 radar imagery from Sentinel-1 (overpass on Jan 19, 2017)

305 **7. CONCLUSIONS AND RECOMMENDATIONS FOR HCFCD**

306 HCFCD has currently developed a system that predicts inundation extent of riverine
307 flooding on real-time basis based on observed gage water surface elevation and effective HEC-
308 RAS model products. This real-time prediction is available for public on Harris County Flood
309 Warning System website (<https://www.harriscountyfws.org>) to notify the people about the extent
310 of the flood during storm event. Therefore, having forecasted water surface elevation can
311 improve decision making involving inundation-forecasting by HCFCD using the existing Flood
312 Inundation Mapping System (FIMS), which is developed for the real-time inundation prediction
313 based on now cast of water levels by gauges. The rating curve based approach yields acceptable
314 skill at 1-4 day lead times and does not require CPU or time-intensive procedures. Thus, these
315 inundation maps can be generated and continuously updated as soon as a new QPF run is
316 complete and provide HCFCD an additional source of information for risk assessment and
317 decision making.

318 In addition to the key finding on the feasibility of the rapid inundation forecasting
319 technique, this research makes the following conclusions for urban flood forecasting:

- 320 1. Affordable CPU resources in the range of 3000-4000 USD should be invested as they are
321 sufficient for quantitative precipitation forecasting up to 72 hours or more. An alternate
322 option is to leverage the power of cloud computing services now being offered by various
323 vendors such as Google Earth engine and Amazon web services at a low price.
- 324 2. Since, hurricane strength storm forecasting using GFS downscaling is challenging
325 without adequate calibration and parameterizations, agencies like HCFCD should also
326 look at rapid refresh cloud motion IR imagery with WRF/GFS forecast for storms while
327 appropriate WRF set up is developed using HWRF.

- 328 3. Moderately intense storms can be forecast by GFS and WRF with much higher skill.
- 329 4. To further improve QPF skill, WRF set up should be calibrated with appropriate
- 330 parameterization selection for Houston – and season (summer and winter) and hurricanes
- 331 using HWRF. In other words, agencies like HCFCD should explore unique WRF setups
- 332 at 1km resolution with differing choice of parameterizations for each flood season.
- 333 5. To further improve water level forecasting skill, unique rating curve between
- 334 precipitation and water level change at a location should be developed for small,
- 335 moderate and heavy storms that trigger differing runoff hydraulics.

336 The goal in this study was to explore the operational feasibility and skill of high-

337 resolution QPF using NWP models for rapid (real-time) urban flood management for the Harris

338 County Flood Control District. Based on a very systematic study using WRF over hurricane and

339 non-hurricane storms using dense gauge network, a path forward for this operational

340 sustainability for HCFCD has been identified. The authors believe that with continued work

341 based on the key conclusions of the study, a flood management agency like HCFCD should be

342 able to add forecast functionality to its inundation mapping capability in a sustainable manner.

343 Consequently, this new functionality should considerably improve decision making to save lives

344 and protect property without adding considerably to operational overhead of the agency.

345 **Acknowledgements:** The authors are thankful to the Harris County Flood Control District

346 (HCFCD) for making the data and information available to us through their flood warning

347 system website. The authors are also grateful to the National Oceanic and Atmospheric

348 Administration (NOAA) for providing a global-scale model based weather forecast data.

349

350 **8. REFERENCES**

- 351 Chen, X., Hossain, F., and Leung, L. R. (2017a). “Establishing a Numerical Modeling
352 Framework for Hydrologic Engineering Analyses of Extreme Storm Events.” *J. Hydrol.
353 Eng.*, 10.1061/(ASCE)HE.1943-5584.0001523, 4017016.
- 354 Chen, X., Hossain, F., and Leung, L. R. (2017b). “Probable Maximum Precipitation in the US
355 Pacific Northwest in a Changing Climate.” *Water Resources Research*, 53(11), 9600-9622,
356 10.1002/2017WR021094.
- 357 Chen, X., and Hossain, F. (2016). “Revisiting extreme storms of the past 100 years for future
358 safety of large water management infrastructures.” *Earth’s Future*, 4(7), 306-322,
359 10.1002/2016EF000368.
- 360 Dodla, V. B., Desamsetti, S., and Yerramilli, A. (2011). “A Comparison of HWRF, ARW and
361 NMM Models in Hurricane Katrina (2005) Simulation.” *Int J Environ Res Public Health*,
362 8(6), 2447–2469, 10.3390/ijerph8062447.
- 363 Durkee, J. D., Campbell, L., Berry, K., Jordan, D., Goodrich, G., Mahmood R., and Foster, S.
364 (2012). “A Synoptic Perspective of the Record 1-2 May 2010 Mid-South Heavy Precipitation
365 Event.” *Bulletin of American Meteorological Society*, 93(5), 611–620, 10.1175/BAMS-D-11-
366 00076.1.
- 367 Emanuel, K. (2017). “Assessing the present and future probability of Hurricane Harvey's
368 rainfall.” *Proceedings of the National Academy of Sciences*, 114 (48), 12681-12684,
369 10.1073/pnas.1716222114.

370 Khan, S. D. (2005). "Urban development and flooding in Houston Texas, inferences from remote
371 sensing data using neural network technique." *Environ Geol*, 47(8), 1120-1127,
372 [10.1007/s00254-005-1246-x](https://doi.org/10.1007/s00254-005-1246-x).

373 Liguori, S., Rico-Ramirez, M. A., Schellart, A. N. A., and Saul, A. J. (2012). "Using
374 probabilistic radar rainfall nowcasts and NWP forecasts for flow prediction in urban
375 catchments." *Atmospheric Research*, 103, 80–95, 10.1016/j.atmosres.2011.05.004.

376 Liu, J., Wang, J., Pan, S., Tang, K., Li, C., and Han, D. (2015). "A real-time flood forecasting
377 system with dual updating of the NWP rainfall and the river flow." *Natural Hazards*, 77(2),
378 1161–1181, 10.1007/s11069-015-1643-8.

379 Rotunno, R., Chen, Y., Wang, W., Davis, C., Dudhia, J., and Holland, G. J. (2009). "Large-eddy
380 simulation of an idealized tropical cyclone." *Bulletin of American Meteorological Society*,
381 90(12), 1783–1788, 10.1175/2009BAMS2884.1.

382 Sikder, M. S., and Hossain, F. (2018). "Improving Operational Flood Forecasting in Monsoon
383 Climates with Bias-corrected Quantitative Forecasting of Precipitation." *International
384 Journal of River Basin Management*, 10.1080/15715124.2018.1476368.

385 Sikder, S., and Hossain, F. (2016). "Assessment of the weather research and forecasting model
386 generalized parameterization schemes for advancement of precipitation forecasting in
387 monsoon-driven river basins." *Journal of Advances in Modeling Earth Systems*, 8(3), 1210-
388 1228, 10.1002/2016MS000678.

389 Skamarock, W. C., Klemp, J. B., Dudhia, J., Gill, D. O., Barker, D. M., Duda, M. G., Hung, X.
390 Y., Wang, W., and Powers, J. G. (2008). "A description of the advanced research WRF
391 Version 3." NCAR Tech. Note NCAR/TN-4751STR. NCAR: Boulder, CO.

392 Zelinski, A., and Zaveri, M. (2018). “Push to solve Houston's chronic flooding grows stronger.”
393 *Houston Chronicle*, February 10, (available:
394 [https://www.houstonchronicle.com/news/houston-texas/houston/article/Nearly-six-months-](https://www.houstonchronicle.com/news/houston-texas/houston/article/Nearly-six-months-after-Harvey-some-traction-for-12567647.php#photo-14028673)
395 [after-Harvey-some-traction-for-12567647.php#photo-14028673](https://www.houstonchronicle.com/news/houston-texas/houston/article/Nearly-six-months-after-Harvey-some-traction-for-12567647.php#photo-14028673); last accessed October 18,
396 2018).
397